Separation Science and Technology
Publication details, including instructions for authors and subscription information:
http://www.informaworld.com/smpp/title~content=t713708471

Fluoride adsorption onto α-Al_2O_3 and its effect on the zeta potential at the alumina-aqueous electrolyte interface

J. L. Reyes Bahena[a]; A. Robledo Cabrera[a]; A. López Valdivieso[b]; R. Herrera Urbina[c]
[a] Universidad Autónoma de San Luis Potosí, San Luis Potosí, SLP, Mexico [b] Universidad Autónoma de San Luis Potosí, San Luis Potosí, Mexico [c] Departamento de Ingeniería Química y Metalurgia, Universidad de Sonora, Hermosillo, Son. Mexico

To cite this Article Bahena, J. L. Reyes , Cabrera, A. Robledo , Valdivieso, A. López and Urbina, R. Herrera(2002) 'Fluoride adsorption onto α-Al_2O_3 and its effect on the zeta potential at the alumina-aqueous electrolyte interface', Separation Science and Technology, 37: 8, 1973 — 1987

To link to this Article: DOI: 10.1081/SS-120003055

URL: http://dx.doi.org/10.1081/SS-120003055

SEPARATION SCIENCE AND TECHNOLOGY, 37(8), 1973–1987 (2002)

FLUORIDE ADSORPTION ONTO α-Al_2O_3 AND ITS EFFECT ON THE ZETA POTENTIAL AT THE ALUMINA–AQUEOUS ELECTROLYTE INTERFACE

J. L. Reyes Bahena,[1] A. Robledo Cabrera,[1]
A. López Valdivieso,[1,*] and R. Herrera Urbina[2]

[1]Instituto de Metalurgia, Universidad Autónoma de San
Luis Potosí, Av. Sierra Leona 550, Lomas 2a Secc, San Luis
Potosí, SLP, Mexico 78210
[2]Departamento de Ingeniería Química y Metalurgia,
Universidad de Sonora, Apartado Postal 106, Hermosillo,
Son. Mexico 83000

ABSTRACT

Fluoride removal from aqueous solutions using α-Al_2O_3 as an adsorbent was investigated through adsorption and electrokinetic studies, using two different initial fluoride concentrations relevant to fluoride contents in drinking water, namely 3 and 10 mg/L. Maximum fluoride removal was achieved between pH 5 and 6 at 25°C. Adsorption at both pH 5 and 9 correlates to the Langmuir isotherm. The point of zero charge (pzc) of α-Al_2O_3 at 20°C was determined using three different concentrations of $NaNO_3$ as an indifferent electrolyte. It was found to occur at pH 9.2. Through mineral/solution equilibria, this pzc was determined to be close to pH 9.5 of minimum solubility of amorphous aluminum hydroxide,

---

[*] Corresponding author. Fax: (52) 48-25-4326; E-mail: alopez@uaslp.mx

www.dekker.com

suggesting the formation of this species onto the adsorbent's surface. Zeta potential of α-Al_2O_3 in the presence of fluoride reversed sign towards more acidic pH values in comparison to the pzc, indicating specific adsorption of fluoride. Fluoride adsorption onto alumina under mildly acidic conditions seemed to involve mainly a replacement of surface OH^- by F^-. Adsorption is small at pH 9 and up to about 10 and it seems to take place through hydrogen bonding.

Key Words: Drinking water defluoridation; Fluoride adsorption; Electrokinetics; Alumina

INTRODUCTION

Maximum allowed fluoride concentration in drinking water ranges from 0.7 to 1.2 mg/L depending on the mean daily air temperature (1). In many parts of the world, however, drinking water contains high levels of fluoride derived from natural sources, and its excessive ingestion constitutes a high health risk that can lead to fluorosis of teeth and bones (2–7). Humans consuming water containing fluoride as low as 4 mg/L over a long period of time can develop fluoride osteoporosis. Defluoridation of water supplies is therefore necessary to avoid health problems associated to fluoride overexposure. Methods for water defluoridation include fluoride precipitation with calcium salts (8) and fluoride adsorption onto various adsorbents: alum sludge (9), alumina (10–12,18), fly ash (13), bone char (14), activated carbon (15), and resins (16).

Excess fluoride has been removed from drinking water using highly porous adsorbents such as activated alumina (10,17,18). This aluminum oxide is a granular material with a large specific surface area, usually between 240 and 300 m^2/g. Churchill (10) was the first to report the use of activated alumina for fluoride removal from drinking water. He found that the best experimental pH values for water treatment were between 5 and 6.5. It has been reported that fluoride removal from solution takes place by an ion exchange mechanism involving the active sites on the surface of alumina (11,12,19). The mechanism of fluoride removal from aqueous solutions using aluminum oxides or hydroxides, however, is not fully understood. To gain a better understanding of the interaction between fluoride and aluminum hydroxides, α-Al_2O_3, a low-porosity aluminum oxide with a small specific surface area was selected as an adsorbent. This research work was undertaken to investigate the effect of pH on fluoride adsorption onto α-Al_2O_3. Electrokinetic experiments were carried out to determine the point of zero charge (pzc) of the adsorbent and for indirect identification of fluoride adsorption mechanisms.

EXPERIMENTAL MATERIALS AND METHODS

The α-Al_2O_3 powder used for both adsorption and electrokinetic experiments was purchased from Taimei Chemicals Co. Ltd. It has a purity of 99.99%, a specific surface area of 17.4 m^2/g, and a mean particle size of 0.15 μm. This alumina sample was selected because of its relatively high acid resistance, which minimizes losses during regeneration, and for its nonporous nature. All chemicals were reagent analytical grade compounds. $NaNO_3$ was used as a supporting electrolyte for maintaining the ionic strength of suspensions constant. Dilute solutions of NaOH and HNO_3 were used for pH adjustments. NaF was used as fluoride source. All solutions and suspensions were prepared with deionized water (resistivity = 17.4 megohm cm at 25°C) obtained with a Barnstead E-pure apparatus.

Alumina suspensions were prepared in polypropylene bottles. Suspensions for electrophoresis measurements in the presence of an indifferent electrolyte were prepared at 20°C as follows: a measured amount of (50 mg) α-Al_2O_3 was added to 100 mL, 0.1 mol/L, 0.01 mol/L or 0.001 mol/L aqueous sodium nitrate, and the suspension was aged for 24 hr at its natural pH. After the aging period, the pH was adjusted to the desired value, and the suspension conditioned further during 30 min. Before filling the electrophoresis cell with the suspension, the pH was recorded and reported as final pH. Electrokinetic measurements were conducted with an electrophoresis unit manufactured by Zeta Meter Inc. At least 10 different particles were tracked for determining the average electrophoretic mobility, which was converted to a zeta potential value through the Henry's equation (20) given by:

$$\zeta = 6\pi\eta \mathrm{EM}/\varepsilon f(\kappa\alpha) \tag{1}$$

where ζ is the zeta potential, η the water viscosity, EM the electrophoretic mobility, ϵ the water dielectric constant, κ the electrical double layer thickness, and α is the particle radius, which was taken as 75 nm. $f(\kappa\alpha)$ values were determined at the various ionic strengths used in this study as described by Hunter (20).

Adsorption experiments were conducted as follows: 500 mg alumina were added to an aqueous solution of 0.01 M $NaNO_3$ containing 3 or 10 mg/L total fluoride, and the pH was adjusted to the desired value. This suspension was equilibrated at 25°C for 24 hr. The pH of this suspension was measured afterwards and reported as final pH. An aliquot was taken and centrifuged at

5000 rpm during 30 min. The solution recovered after centrifugation was used for determining the concentration of total fluoride remaining in the solution. The rest of the suspension was used for electrophoresis measurements in the presence of fluoride in the system.

The total fluoride concentration in the solution was measured with an ion selective electrode connected to an Orion Specific Ion Meter Model SA-720 and coupled to a standard calomel electrode as reference. The range of fluoride concentrations that can be analyzed by this technique varies from 0.1 to 1000 mg/L. For avoiding interference with the electrode performance, an ionic strength fixer and buffer solution [TISAB: 1 *M* NaCl + 1 *M* acetic acid + 1 *M* CDTA, (1,2 cyclohexylenediamine tetraacetic acid)], set to a pH in the range of 5.0–5.3 with 6 N NaOH was added during actual measurements (21). A given volume of TISAB solution was added to a volume of fluoride-containing supernatant and allowed to stand for 2 hr at 25°C before reading the electromotive force of the electrode.

RESULTS AND DISCUSSION

Determination of the Point of Zero Charge of α-Al_2O_3

Adsorption from solution at the solid–aqueous electrolyte interface is affected by the interfacial electrical characteristics of the substrate, which can be assessed by electrokinetic measurements. This experimental technique has also been used to investigate adsorption phenomena for indirect identification of adsorption mechanisms, and it has proven to be a very reliable technique for measuring electrical effects at the interface caused by the adsorption of ions. From electrokinetic results, one can determine the single most important parameter that represents the electrical nature of the oxide–aqueous electrolyte interface, pzc. In the case of oxides, the pzc is given by the proton condition in solution at which the surface charge caused by H^+ or OH^- binding is zero. In the absence of ions adsorbed specifically, other than H^+ and OH^-, the pzc coincides with the isoelectric point, which is the pH of zero electrokinetic potential (22).

The electrokinetic behavior of α-Al_2O_3 in aqueous suspensions containing indifferent electrolytes has been amply investigated. In this research work, the pzc of α-Al_2O_3 was determined from the electrophoresis results shown in Fig. 1, which shows zeta potential–pH curves for three different concentrations of $NaNO_3$. Since the three curves intersect at a common single point that also corresponds to zero zeta potential, namely pH 9.2, the pzc of α-Al_2O_3 occurs at this pH. These results also indicate that Na^+ and NO_3^- are indifferent counterions for this oxide. The pzc values reported for α-Al_2O_3 are pH 9.0 (23) and pH 9.1 (24–26). The dissociation of the hydrated surface of α-Al_2O_3 to yield a positively

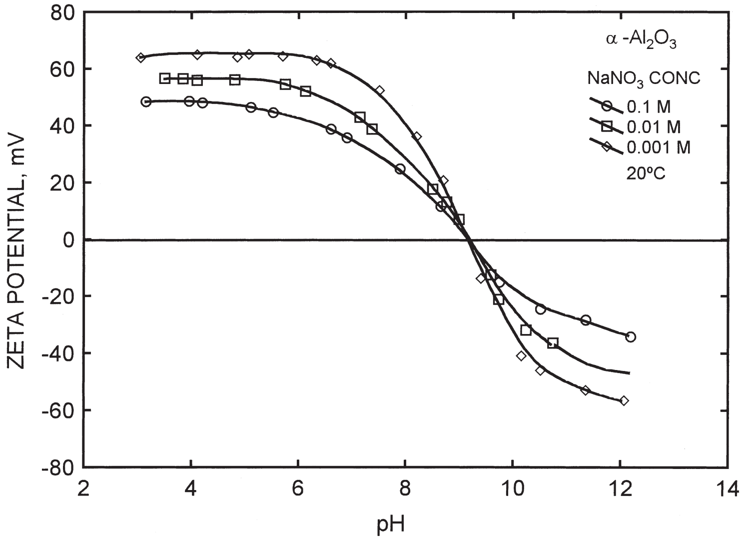

Figure 1. The zeta potential of α-Al$_2$O$_3$ as a function of pH at 20°C and three different concentrations of NaNO$_3$.

charged or negatively charged surface may be given by (27,34):

$$\mathrm{Al(OH)\,(surf) + H^+ = Al(OH)_2^+(surf)} \tag{2}$$

$$\mathrm{Al(OH)\,(surf) + OH^- = AlO^-(surf) + H_2O} \tag{3}$$

The pzc for oxides represents the point at which the positively charged surface site density equals that of the negative sites. This pzc has been related to the pH at which the oxide shows its minimum solubility (27). To determine the theoretical pH of minimum solubility of alumina, computations of solid–solution equilibria were carried out as a function of pH using the available thermodynamic data for the α-Al$_2$O$_3$–H$_2$O system (22,25,28). The results of these computations were then used to construct the solubility curve as a function of pH given in the logarithmic plot shown in Fig. 2, which clearly indicates a minimum solubility at about pH 7. This pH value, however, does not correspond to the pzc of α-Al$_2$O$_3$ determined by electrophoresis. This discrepancy can be explained in terms of the extent of surface hydration of the alumina sample used in this investigation. Since the aqueous alumina suspensions were aged for 24 hr prior to the electrokinetic experiments, its surface must be extensively hydrated and even covered by an aluminum hydroxide layer. Computations of solid-solution equilibria were also carried out for both crystalline Al(OH)$_3$–water and amorphous Al(OH)$_3$ –water

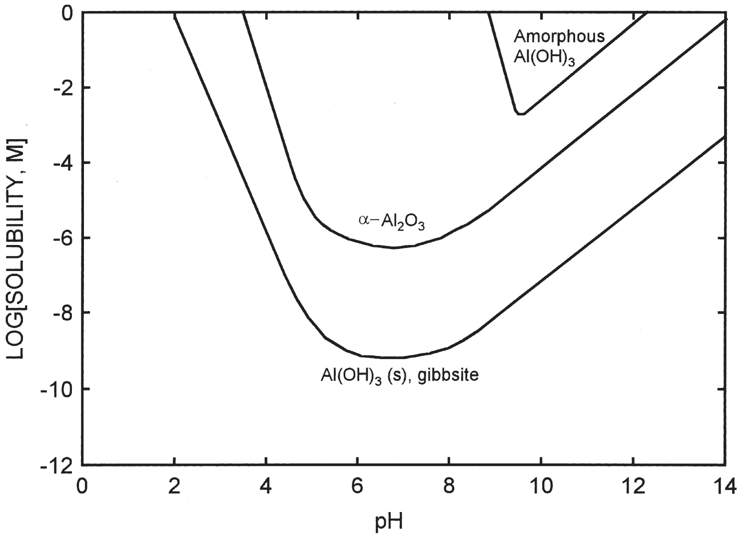

Figure 2. Equilibrium solubility of α-Al_2O_3, crystalline $Al(OH)_3$, gibbsite, and amorphous $Al(OH)_3$, as a function of pH at 25°C and zero ionic strength.

systems. The solubility curves constructed from these results as a function of pH are also shown in Fig. 2. These curves clearly show that the crystalline form of $Al(OH)_3$, gibbsite, also exhibits a solubility minimum at about pH 7, and it is more insoluble than both α-Al_2O_3 and amorphous $Al(OH)_3$. In addition, they clearly indicate that amorphous $Al(OH)_3$ in equilibrium with its solution is the most soluble phase and exhibits a solubility minimum at pH 9.5, a value close to the pHpzc of α-alumina determined from electrokinetic experiments. Zeta potential measurements and solid-solution equilibria substantiate the assumption that the surface of aged alumina seems to be coated by amorphous $Al(OH)_3$. Classical thermodynamics, on the other hand, indicate that the more insoluble gibbsite phase should form on the surface of aged alumina in aqueous suspensions. Parsons' results (29), however, have confirmed the preferential formation of amorphous phases on the surface of metallic oxides. In the case of α-alumina, amorphous $Al(OH)_3$, instead of crystalline gibbsite, has been reported to form on its surface (25).

The pH of minimum solubility of a metallic oxide in equilibrium with an aqueous solution has been found to correspond to the pH at which the solution is electrically neutral with respect to the concentration of positive and negative metal–hydroxo complexes. The pH at which this condition is satisfied gives the isoionic point (iip) of the solution. From computations of amorphous $Al(OH)_3$–

solution equilibria as a function of pH, a solubility diagram was constructed and it is presented in Fig. 3. This figure gives the concentration of free aquo Al(III) and hydroxo–aluminum complexes in equilibrium with $Al(OH)_3$, and clearly shows that the iip closest to the pH of minimum solubility of the solid is given by the condition $5[Al_{13}(OH)_{34}^{5+}] = [Al(OH)_4^-]$, which occurs at pH 9.3. This iip value is very close to both the pH of minimum solubility of the hydroxide and the pzc of α-Al_2O_3 determined from electrophoresis. The solubility curve of amorphous $Al(OH)_3$ is also presented in this figure for comparison.

Kinetics of Fluoride Removal by α-Al_2O_3 from Aqueous Electrolytes

For determining the equilibrium time for the removal of fluoride from aqueous solutions using α-Al_2O_3 as an adsorbent, kinetics experiments were performed at mildly acidic pH values, using solutions with fluoride concentrations relevant to those encountered in some drinking waters. Results indicate a fast adsorption step at short contact times and a slow process after about one hour. Similar adsorption kinetics has been reported for the removal of fluoride from

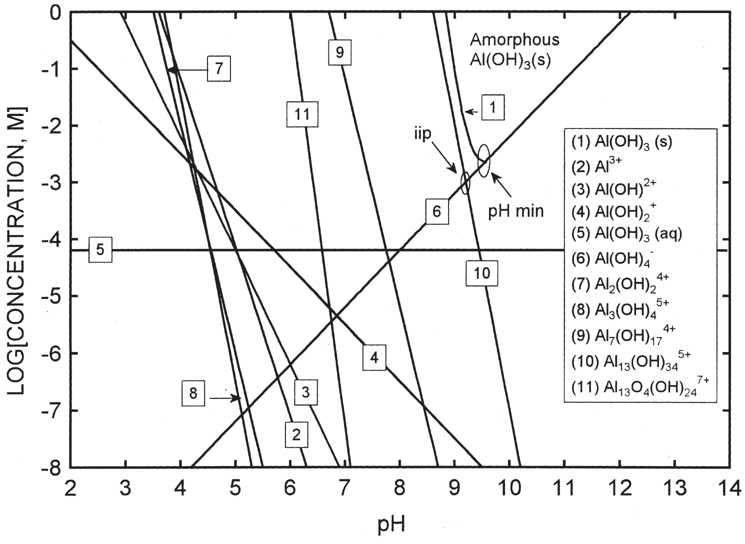

Figure 3. Solubility diagram of amorphous $Al(OH)_3$ as a function of pH at 25°C and zero ionic strength. The numbers on the lines refer to the corresponding ionic species in solution. pHmin indicates the minimum solubility of amorphous alumina, iip is the isoionic point of the solution in equilibrium with amorphous alumina.

aqueous solutions using alum sludge (9). For solutions containing 3 mg/L initial fluoride, fluoride removal from solution after 1.3 hr was 58.8% at pH 5.2, 56.6% at pH 4.4, and 50.7% at pH 6.7. The uptake process continues slowly with time and reaches 64.5% at pH 5.2, 57.6% at pH 4.4, and 55.9% at pH 6.7 after 24 hr. When initial fluoride is increased to 10 mg/L, the best conditions for fluoride uptake are at pH 5.7. At pH 4.8, 28.5% fluoride removal is achieved after 1.3 hr and 33.5% after 24 hr; 22.5% fluoride is removed after 1.3 hr and 30.5% after 24 hr at pH 6.8. The loading capacity of α-Al_2O_3 was found to increase with increasing initial fluoride concentration. According to these results, it was decided to equilibrate the α-Al_2O_3-aqueous fluoride suspension during 24 hr for conducting electrokinetics and adsorption experiments as a function of pH.

Effect of Fluoride on the Zeta Potential of α-Al_2O_3

Zeta potential results of α-Al_2O_3 in the absence and presence of various initial fluoride concentrations are shown in Fig. 4 as a function of pH. This figure shows that as the initial fluoride concentration increases, the isoelectric point of the oxide adsorbent shifts to lower pH values and the zeta potential becomes more negative in the pH range 3–10. This electrokinetic behavior is typical of

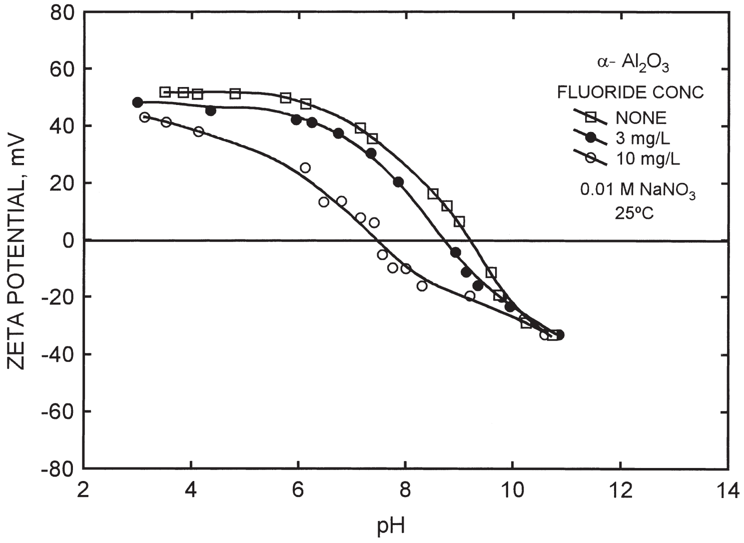

Figure 4. The zeta potential of α-Al_2O_3 as a function of pH at 25°C and 0.01 *M* $NaNO_3$ in the absence and presence of different fluoride concentrations.

systems where an ion adsorbs specifically. In the case of alumina, it seems to be mainly related to the adsorption of free fluoride, which can exchange with surface OH groups, as recently shown by 19F NMR spectroscopy of Aluminum hydro(oxides) in fluoride solutions (30). Below the pHpzc, the adsorption of fluoride on positively charged surface hydroxyl groups may be written as:

$$AlOH_2^+(\mathrm{surf}) + F^- = AlF(\mathrm{surf}) + H_2O \tag{4}$$

This reaction explains the decrease in positive zeta potentials measured under these conditions. In addition, the replacement of a surface OH by F suggests that all F charge (-1) is located at the surface (31), which is in agreement with the zeta potentials measured at the α-alumina–aqueous fluoride interface in this investigation.

Computations of solution equilibria were carried out as a function of pH using the available thermodynamica data for the Al(III) –F–H_2O system (19). These results were then used to construct speciation diagrams of the type shown in Fig. 5, corresponding to 8×10^{-5} mol/L total Al(III) and 2×10^{-4} mol/L total fluoride. This diagram reveals that aluminum–fluoro complexes predominate in solution below about pH 6.0. In neutral and basic solutions, hydroxide ligands compete with fluoride for the aluminum cation. As a result, aluminum hydroxide precipitates from solution and aluminum–hydroxo complexes predominate in solution.

Effect of PH on the Adsorption of Fluoride onto α-Al_2O_3

The effect of pH on the adsorption density of fluoride onto α-Al_2O_3 after 24 hr equilibration with aqueous solutions containing 3 and 10 mg/L initial fluoride is shown in Fig. 6. These concentrations were used as they lead to fluorosis of teeth and bones when such levels are present in drinking waters (2–7). Fluoride adsorption densities were calculated using the difference between added fluoride and the total fluoride concentration remaining in the solution after the reaction time. Maximum fluoride adsorption density was found to occur between pH 5 and 6 for the two initial fluoride concentration, in agreement with the findings of Clifford et al. (17), and Churchill (10). In both concentrations, fluoride adsorption density drops drastically above pH 6 and it also decreases at pH values below those at which adsorption is maximum. The deleterious effect of acid solutions on fluoride adsorption may be related to an increase in the solubility of α-Al_2O_3 under these conditions, as shown by its solubility curve shown in Fig. 2. This curve clearly shows that the solubility of α-Al_2O_3 increases significantly as the pH decreases below about pH 5. In addition, as is well known, the solubility of finely divided solids is significantly higher than that of their massive forms (32). Al(III) dissolved from the crystal lattice of alumina will be

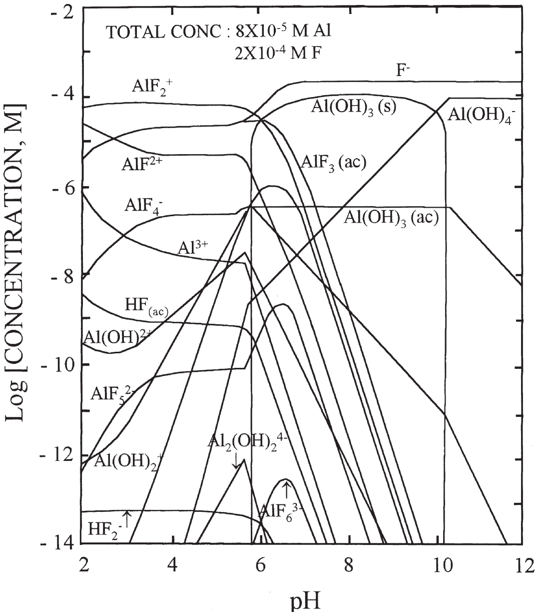

Figure 5. Speciation diagram for the Al(III)–F(I)–H_2O system. Total aluminum concentration is 8×10^{-5} *M* and total fluoride concentration is 2×10^{-4} *M*.

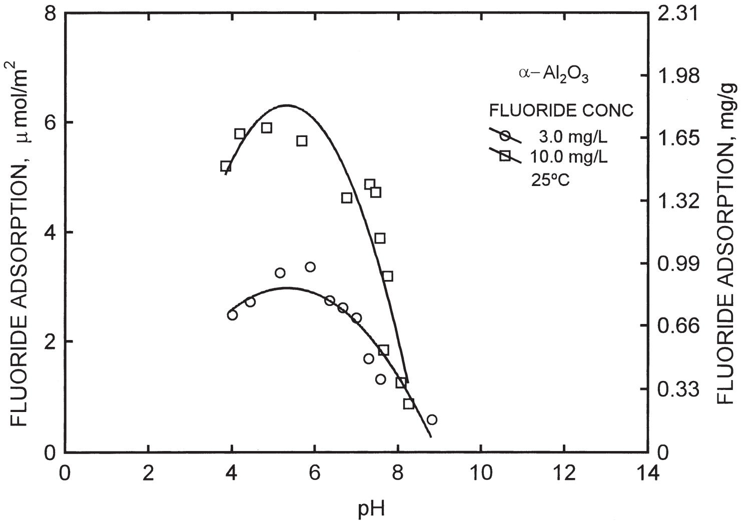

Figure 6. Adsorption of fluoride onto α-Al_2O_3 as a function of pH at 25°C and 0.01 *M* $NaNO_3$, with two different initial concentrations of fluoride.

complexed by the fluoride ligand forming aluminum–fluoro complexes in solution, which predominate below about pH 6 (see Fig. 5). Fluoride has been found to promote the dissolution of aluminum hydro(oxides) at pH 5.0 (30). The decrease in fluoride adsorption as the pH increases above 6 can be related to two factors, namely the aluminum–hydroxo complex species being more stable on the alumina's surface than the aluminum–fluoro complexes, and the electrotatic repulsion between the fluoride and the surface owing to their similarity in negative charge.

Adsorption Isotherms

Isotherms of fluoride adsorption onto α-Al_2O_3 at pH 5 and 9 are shown in Fig. 7. These results were analyzed using both the Freundlich and Langmuir equations, finding that the Langmuir equation gave the best correlation, in agreement with the results of Wu and Nitya (11) on the adsorption of fluoride onto activated alumina. The Langmuir isotherm is given by:

$$\Gamma = \Gamma_m kc/(1 + kc) \tag{5}$$

where Γ is the adsorption density of fluoride on α-Al_2O_3 at the equilibrium fluoride concentration c in the aqueous solution, Γ_m the monolayer coverage, and k is related to the equilibrium constant for the adsorption process. Table 1 shows the values of Γ_m and k at pH 5 and 9 for the isotherms shown in Fig. 7.

Adsorption of fluoride is small at pH 9 (2.13 μmol/m^2), compared to pH 5, where the adsorption would reach a maximum fluoride density of 8.26 μmol/m^2 (2.73 mg F^-/g Al_2O_3). The adsorption capacity at pH 5 is relatively low compared to that of 12.2 mg F^-/g Al_2O_3 reported for activated Al_2O_3, a high specific surface area and high porosity alumina (18). Referring to Fig. 4, it is apparent that adsorption of low magnitude proceeds up to about pH 10 as shown by the decrease in the zeta potential of α-Al_2O_3 in the presence of fluoride ions. At pH 9, very close to the pzc, the electrostatic contribution to the total free

Table 1. Values of Monolayer Coverage (Γ_m) and Constant k for the Langmuir Adsorption Isotherm of Fluoride onto α-Al_2O_3 at pH 5 and 9

pH	Γ_m (μmol/m^2)	k (L/mol)
5	8.26	8529.26
9	2.13	33.12

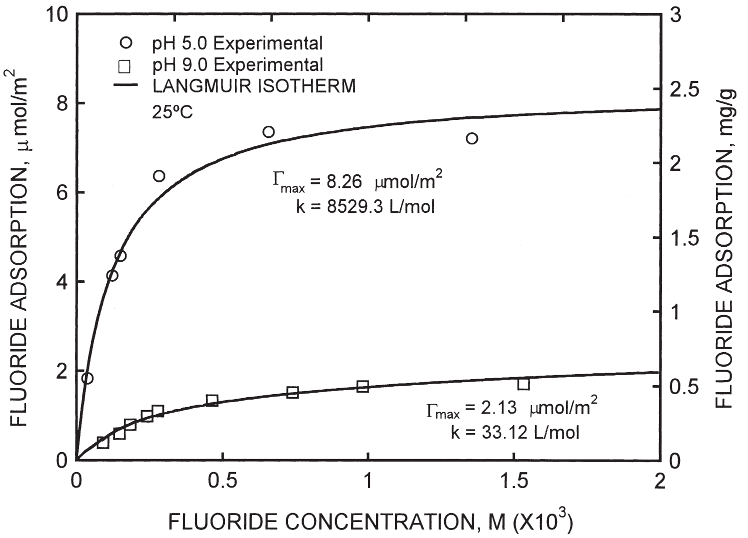

Figure 7. Surface adsorption density of fluoride onto α-Al_2O_3 as a function of equilibrium fluoride concentration at pH 5.0 and 9.0. The experimental and Langmuir equation results.

energy of adsorption must be very small and fluoride adsorption can be attributed to specific adsorption through fluoride hydrogen bonding with surface hydroxyl groups. Aluminum–fluoro complex species do not likely form on the surface of α-Al_2O_3 at pH values close to the pzc and above since aluminum–hydroxo complex species are thermodynamically more stable, as can be seen in the speciation diagram shown in Fig. 5. At pH values above the pzc, hydrogen bonding can also be accounted for fluoride adsorption on the negative surface of α-Al_2O_3 through interaction with uncharged Al(OH) groups, present on the surface in equilibrium with negative AlO^- groups as shown by Eq. (3). At pH values higher than 10, where the zeta potential of α-Al_2O_3 is not affected by fluoride ions, electrostatic repulsion between the negative charged surface and fluoride anions must overcome the interaction due to hydrogen bonding, resulting in no adsorption of fluoride. Fluoride adsorption onto kaolinite has also been explained in terms of both anion exchange and hydrogen bonding (33).

CONCLUSIONS

Fluoride adsorption onto α-Al_2O_3 is very fast during the first 60 min of reaction and continues slowly for up to 24 hr. Maximum fluoride uptake by α-

Al_2O_3 was found to occur between pH 5 and 6 for 3 and 10 mg/L initial fluoride concentration. Above these pH values, fluoride adsorption falls off sharply and it is small at the point of zero charge of the adsorbent occurring at pH 9.2. Zeta potential measurements indicate that fluoride adsorbs specifically onto α-Al_2O_3 by a mechanism that replaces OH^- from positively charged surfaces and through hydrogen bonding under conditions close and above to the pHpzc.

ACKNOWLEDGMENTS

The authors thank the financial support by FAI-UASLP contract No. COO-FAI-07-21.60 and SIHGO contract No. MT-17/96 for this research work. This acknowledgment is extended to Prof. Fernando Díaz Barriga for the measurement of fluoride concentration in his laboratory.

REFERENCES

1. Department of Health and Human Services (DHHS), *Review of Fluoride: Benefits and Risks*; Department of Health and Human Services (DHHS): Washington, DC, 1991.
2. Chen, Y.X.; Lin, M.Q.; He, Z.L.; Xiao, Y.D.; Chen, C.; Min, D.; Liu, Y.Q.; Yu, M.H. Relationship Between Total Fluoride Intake and Dental Fluorosis in Areas Polluted by Airborne Fluoride. Fluoride **1996**, *29* (1), 7–12.
3. Calderón, J.; Romieu, I.; Grimaldo, M.; Hernández, H.; Díaz Barriga, F. Endemic Fluorosis in San Luis Potosí, México. II. Identification of Risk Factors Associated with Occupational Exposure to Fluoride. Fluoride **1995**, *28* (4), 203–208.
4. Díaz Barriga, F.; Leyva Ramos, R.; Quistián, J.; Loyola Rodríguez, J.P.; Pozos, A.; Grimaldo, M. Endemic Fluorosis in San Luis Potosí, México. IV. Sources of Fluoride Exposure. Fluoride **1997**, *30* (4), 219–222.
5. Kahama, R.W.; Kariuki, D.N.; Njenga, L.W. Fluorosis in Children and Sources of Fluoride Around Lake Elementaite Region of Kenia. Fluoride **1997**, *30* (1), 19–25.
6. Grimaldo, M.; Turrubiartes, F.; Milan, J.; Pozos, A.; Alfaro, C.; Díaz Barriga, F. Endemic Fluorosis in San Luis Potosí, México. III. Screening for Fluoride Exposure with a Geographic Information System. Fluoride **1997**, *30* (1), 33–40.
7. Ortiz, D.; Castro, L.; Turrubiartes, F.; Milan, J.; Diaz Barriga, F. Assessment of the Exposure to Fluoride from Drink Water in Durango, México, Using a Geographic Information System. Fluoride **1998**, *31* (4), 183–187.

8. Zabban, W.; Jewett, H.W. The Treatment of Fluoride Wastes. *Proceedings 23rd Purdue Industrial Waste Conference, May, 1967*; No. 2–4, 706–715.
9. Sujana, M.G.; Thakur, R.S.; Rao, S.B. Removal of Fluoride from Aqueous Solution by Using Alum Sludge. J. Colloid Interface Sci. **1998**, *206* (1), 94–101.
10. Churchill, H.V. *Draft Analytical Report—New Orleans Area Water Supply Study—USEPA 906/10-74-002 Lower Mississippi River facility, Slidell*; La. Surveillance and Analysis Div. Región 6: Dallas, TX, 1974.
11. Wu, Y.C.; Nitya, A. Water Defluoridation with Activated Alumina. J. Environ. Eng. Div. **1979**, *105*, 357–367.
12. Schoeman, J.J.; Botha, G.R. Evaluation of the Activated Alumina Process for Fluoride Removal from Drinking Water and Some Factors Influencing This Performance. Water, S A **1985**, *11* (1), 25–32.
13. Piekos, R.; Paslawska Fluoride Uptake Characteristics of Fly Ash. Fluoride **1999**, *32* (1), 14–19.
14. He, G.L.; Cao, S.R. Assesment of Fluoride Removal from Drinking Water by Calcium Phosphate System. Fluoride **1996**, *29* (4), 212–216.
15. Choi, W.W.; Chen, K.Y. The Removal of Fluoride from Waters by Adsorption. J. Am. Water Works Assoc. **1979**, *71*, 562–570.
16. Staebler, C.J. *Journal Treatment and Recovery of Fluoride Industrial Wastes*; EPA-660/2-73-024 U.S. Environmental Protection Agency, 1974.
17. Clifford, D.; Matson, J.; Kennedy, R. Activated Alumina: Rediscovered Adsorbent for Fluoride, Humic Acids and Silica. Ind. Water Eng. **1978**, *15*, 6–12.
18. Leyva Ramos, R.; Juárez Martínez, A. Adsorción de Fluoruros en Varios Tipos Comerciales de Alumina Activada. Avances en Ingeniería Química **1991**, 107–111.
19. Berendeeva, V.L.; Vakhin, I.G.; Goronovskii, I.T. Use of type A-1 Activated Aluminum Oxide for Defluoration of Water. Sov. J. Water Chem. Technol. **1985**, *7* (3), 121–123.
20. Hunter, R.J. *Zeta Potential in Colloid Science*; Academic Press: New York, 1981.
21. Anonymous; Standard Methods for the Examination of Water and Wastewater. Fluoride; American Public Health Association, 1989; 4.84–4.93.
22. Stumm, W.; Morgan, J.J. *Aquatic Chemistry. An Introduction Emphasizing Chemical Equilibria in Natural Waters*, 2nd Ed.; John Wiley and Sons: New York, 1981.
23. Ross, S.; Morrison, I.D. *Colloidal Systems and Interfaces*, 1st Ed.; John Wiley Interscience: New York, 1988.
24. Halter, W.E. Surface Acidity Constants of α-Al_2O_3 between 25 and 70°C. Geochim. Cosmochim. Acta **1999**, *63* (19–20), 3077–3085.

25. Jenkins, D.; Snoeyink, V.L. *Química del Agua*; LIMUSA, S.A.: México, 1990.
26. Yopps, J.A.; Fuerstenau, D.W. The Zero Point of Charge of α-Alumina. J. Colloid Interface Sci. **1964**, *19*, 61–71.
27. De Bruyn, P.L.; Agar, G.E. Surface Chemistry of Flotation. In *Froth Flotation, 50th Anniversary*; Fuerstenau, D.W., Ed.; AIME: New York, 1962; 91–138.
28. Parks, G.A. Free Energies of Formation and Aqueous Solubilities of Aluminum Hydroxide and Oxide Hydroxides at 25°C. Am. Mineral. **1972**, *57*, 1163–1189.
29. Parsons, R. The Electric Double Layer at the Solid-Solution Interface. In *Aquatic Surface Chemistry*; Stumm, W., Ed.; John Wiley Interscience: New York, 1987; 33–48.
30. Nordin, J.P.; Sullivan, D.J.; Phillips, B.L.; Casey, W.H. Mechanisms for Fluoride-Promoved Dissolution of Bayerite [β-$Al(OH)_3(s)$] and Boehmite[γ-AlOOH]: F-^{19}NMR Spectroscopy and Aqueous Surface Chemistry. Geochim. Cosmochim. Acta **1999**, *63* (21), 3513–3524.
31. Hiemstra, T.; Van Riemsdijk, W.H. Fluoride Adsorption on Goethite in Relation to Different types of Surfaces Sites. J. Colloid Interface Sci. **2000**, *225*, 94–104.
32. Hiemenz, P.C.; Rajagopalan, R. *Principles of Colloid and Surface Chemistry*, 3rd Ed.; Marcel Dekker: New York, 1997.
33. Weerasooriya, R.; Wickramarathna, H.U.S. Modeling Anion Adsorption on Kaolinite. J. Colloid Interface Sci. **1999**, *213* (2), 395–399.
34. Fuerstenau, D.W.; Raghavan, S. Some Aspects of the Thermodynamics of Flotation. In *Flotation*; A.M. Gaudin Memorial Volume, Fuerstenau, M.C., Ed.; AIME: New York, 1976; Vol. 1, 21–65.

Received October 2000
Revised September 2001